Eur. Phys. J. B **16**, 355–359 (2000)

THE EUROPEAN PHYSICAL JOURNAL B

EDP Sciences

Raman scattering of Ge dot superlattices

A. Milekhin[1,2,a], N.P. Stepina[2], A.I. Yakimov[2], A.I. Nikiforov[2], S. Schulze[1], and D.R.T. Zahn[1]

[1] Institut für Physik, Technische Universität Chemnitz, 09107 Chemnitz, Germany
[2] Institute of Semiconductor Physics, 630090, Novosibirsk, Russia

Received 25 January 2000

Abstract. Self-organised Ge dot superlattices grown by molecular beam epitaxy of Ge and Si layers utilizing Stranski-Krastanov growth mode were investigated by Raman spectroscopy. An average size of Ge quantum dots was obtained from transmission electron microscopy measurements. The strain and interdiffusion of Ge and Si atoms in Ge quantum dots were estimated from the analysis of frequency positions of optical phonons observed in the Raman spectra. Raman scattering by folded longitudinal acoustic phonons in the Ge dot superlattices was observed and explained using of elastic continuum theory.

PACS. 78.66.Db Elemental semiconductors and insulators – 78.30.Am Elemental semiconductors and insulators – 63.22.+m Phonons in low-dimensional structures and small particles

1 Introduction

Semiconductor zero-dimensional (0D) structures have attracted growing interest because they show optical and electronic properties much different from bulk solid state materials [1,2]. A number of techniques such as quantum dot formation in solvents [3], in glasses [4], through colloidal chemistry [5] was used for the fabrication of these structures. Recently, molecular beam epitaxy (MBE) of several combinations of lattice mismatched materials such as InGaAs/GaAs, InP/InGaP, Si/Ge in Stranski-Krastanov growth mode has lead to self-assembling of quantum dots (QD's) [6]. At the same time the understanding of optical phenomena in the structures with QDs still requires significant theoretical and experimental effort. It is expected that these periodical structures containing QDs combine the properties of 0D and 2D systems. The self-assembling growth of Ge dot superlattice is considered as an effective method for the design of optoelectronic devices due to its compatibility with silicon technology.

Recently, it has been established that Stranski-Krastanov growth mode leads to formation of pseudomorphic Si/Ge 2D systems (superlattices) at the nominal thickness of Ge $d_1 \leq 6$ Å while the growth of the strained dislocation- free Ge QD superlattices was found to be predominant up to a nominal thickness of 20 Å [7]. Further increasing thickness causes a strain relaxation in the structure with an appearance of mismatch dislocations.

In this paper we report on Raman studies of self-organised Ge dot superlattices.

[a] e-mail: a.milekhin@physik.tu-chemnitz.de

2 Experimental details

Samples were grown by MBE on (001)-oriented Si substrates covered by 200 Å Si buffer layer. The growth temperature of the silicon layers was 800 and 500 °C before and after deposition of Ge layer, respectively. The Ge quantum dot layers were grown at 300 °C. The set of samples under investigation consists of Ge and Si layers with nominal thicknesses presented in Table 1. The samples C and K were delta-doped with boron atoms ($N_B = 3 \times 10^{11}$ cm^{-2}) in the middle of 200 Å Ge layers.

For the characterisation of structural parameters of QD's high-resolution transmission electron microscopy (HRTEM) measurements were performed. The HRTEM images were obtained using a transmission electron microscope CM20 FEG Philips with Gatan imaging filter GIF 200.

The Raman scattering experiments were performed at $T = 80$ K using the 514.5 nm line of an Ar^+ with a power of 100 mW. The scattered light was analysed in a backscattering geometry using a Dilor XY triple monochromator equipped with a CCD camera for multichannel detection. The scattering geometries employed were $z(xx) - z$ and $z(xy) - z$ with x, y, z parallel to the [100], [010] and [001] directions, respectively. The resolution was 2.9 cm^{-1} over the whole spectral range.

3 Results and discussion

In order to validate the formation of quantum dots cross-sectional HRTEM experiments were performed. A HRTEM image of sample I which is considered as a typical Ge QD superlattice is presented in Figure 1. Even though

Table 1. Sample description.

Sample Notation	Nominal thickness of Ge layer, d_1/Å	Nominal thickness of Si layer, d_2/Å	Number of periods	Doping existence
A	6	100	10	-
B	11	100	10	-
C	11	200	10	δ-doping $N_B = 3 \times 10^{11}$ cm^{-2}
D	14	15	10	-
E	14	25	10	-
F	14	45	10	-
I	14	125	10	-
K	14	200	10	δ-doping $N_B = 3 \times 10^{11}$ cm^{-2}

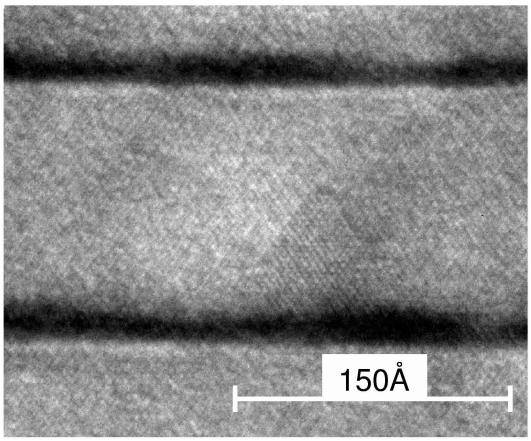

Fig. 1. HRTEM image of the sample I. Light region show the Si layers, dark regions are the Ge dot layers.

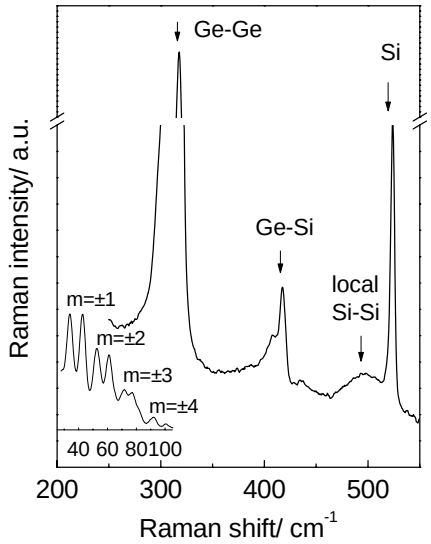

Fig. 2. Typical Raman spectrum of the Ge dot superlattices (sample I) measured in $z(xx) - z$ geometry at a temperature of 80 K. The inset shows the acoustic folded doublets.

the high density of Ge QDs in the layer overlapping in the HRTEM picture prevents the distinct observation of single QDs the dot base size was found to be approximately 15 nm with a QD height of 1.5 nm. Similar samples without Si cap layer were also examined *ex situ* with scanning tunneling microscopy [8] and show the same structural parameters of QDs. The quantum dots are pyramidal with base orientation along [100] and [010] directions. The side facets are formed by {105} planes. The real density of the dots was estimated to be 3×10^{11} cm^{-2}. The dot uniformity is about 20%.

A typical Raman spectrum of Ge dot superlattice is shown in Figure 2. The strong peaks in the spectrum at 319, 417 and 522 cm^{-1} correspond to Ge- Ge, Ge-Si vibrational modes and the Si phonon predominantly from the substrate, respectively. The broad feature at 494 cm^{-1} is attributed to local Si-Si vibrations in the SiGe alloy formed at the interface. The shoulder at about 410 cm^{-1} will be discussed later on. The inset to the figure shows the Raman spectrum in the low frequency spectral range where four doublets ($m = \pm 1, \pm 2, \pm 3, \pm 4$) with decreasing intensities can be seen. These doublets were assigned to scattering by folded longitudinal acoustic (LA) phonons. They result from the artificially introduced periodicity d along the growth direction. Similar features have been investigated in semiconductor superlattices with continuous 2D layers [9–11]. The new periodicity produces a Brillouin minizone (with the maximum wave vector at the zone edge of $q_{\max} = \frac{\pi}{d}$) much smaller than the initial Brillouin zone (with $q_{\max} = \frac{\pi}{a}$, where a is the lattice parameter). The resulting acoustic phonon dispersion can be obtained by the folding of original dispersion curve into

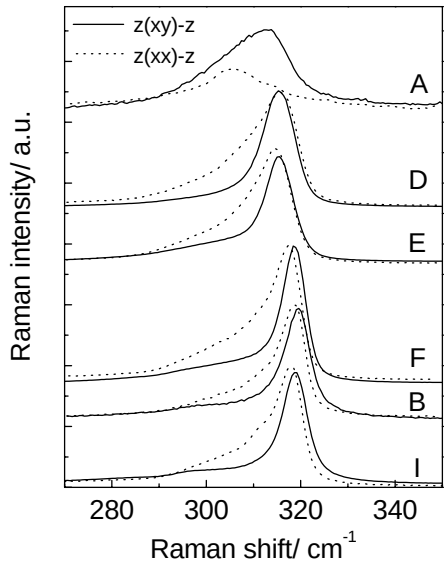

Fig. 3. Raman spectra of the samples A-I measured in $z(xy)-z$ and $z(xx)-z$ geometries in the spectral range of the Ge optical vibrations (solid and dotted lines, respectively) at a temperature of 80 K.

the minizone. The acoustic phonon dispersion curves in the structure and thus the doublet frequency position can be calculated using the elastic continuum model [12]:

$$\cos(qd) = \cos\left(\frac{\omega d_1}{\nu_1}\right)\cos\left(\frac{\omega d_2}{\nu_2}\right) - \frac{k^2+1}{2k}\sin\left(\frac{\omega d_1}{\nu_1}\right)\sin\left(\frac{\omega d_2}{\nu_2}\right) \qquad (1)$$

where $k = \dfrac{\nu_1\rho_1}{\nu_2\rho_2}$; $d = d_1 + d_2$; d_1 and d_2, ρ_1 and ρ_2, ν_1 and ν_2 are the thickness, density and sound velocity in Ge and Si layers, respectively.

Let us consider optical and acoustic spectral regions in detail.

3.1 Optical region

Figure 3 shows Raman spectra of the samples under investigation in the spectral range of optical phonons in Ge measured in different scattering geometries. According to the selection rules for Raman scattering for these superlattices the odd confined longitudinal optical (LO) phonons can be seen in $z(x,y)-z$ scattering geometry while only LA phonons are observable in $z(x,x)-z$ geometry. The dominant feature in the Raman spectrum of sample A measured in $z(x,y)-z$ geometry was attributed to the first confined (LO_1) phonon within Ge dot layer. The Raman peak at 307 cm^{-1} observed in $z(x,x)-z$ geometry is interpreted as second-order scattering by 2TA phonons originating from the X or (and) Σ points of the Brillouin zone in Si layers or (and) Si bulk [13]. The broad shoulder observed in the spectra of all samples measured in $z(x,x)-z$ geometry at the same frequency confirms this interpretation. For the samples B-K where the formation of QDs is expected the selection rules valid for Si/Ge superlattice are not any more fulfilled. Raman spectra of these samples reveal the LO_1 phonons in $z(x,x)-z$ geometry. One can see from Figure 3 that the frequency position of the Ge optical phonon is shifted towards higher frequencies with respect to its bulk value (304 cm^{-1}) up to 11 cm^{-1} and 15 cm^{-1} for samples A, D, E and F, B, I respectively. At least three physical origins can cause a frequency shift of optical phonons.

One of the reason for a shift towards higher frequency is strain in Ge. The lattice mismatch of Ge and Si lattice parameters leads to a tensile strain in z direction and a compressive strain in the xy plane. The strain-induced shift of the optical phonon frequency position can be estimated by the equation [14]

$$\Delta\omega = \frac{1}{2\omega}[p\varepsilon_{zz} + q(\varepsilon_{xx}+\varepsilon_{yy})] = 17\ cm^{-1}, \qquad (2)$$

where ω is the frequency of optical phonon in bulk Ge, p, q are the deformation potentials of the optical phonon in Ge, ε_{xx}, ε_{yy}, ε_{zz} are the diagonal components of the strain tensor. The parameters further used in the calculation were taken from reference [15].

A second reason for a shift but in an opposite direction is the confinement effect of optical phonons which is rather well investigated and understood in semiconductor superlattices [16]. The spatial limitations of SL layers cause a shift of optical phonons towards lower frequency. The confinement effect is most pronounced for sample A with the minimal thickness of the Ge layer. However, the shift due to confinement determined from the dispersion of optical phonons in Ge does not exceed 5 cm^{-1}. The influence of confinement effect is not significant for the other samples. Due to larger nominal thickness of the Ge layers this shift should be about 2 cm^{-1} because of a rather flat dispersion of Ge optical phonons near the centre of the Brillouin zone. Moreover, due to Ge QD formation the real height of QD exceeds the "nominal" value which leads to further reduction of the confinement-induced shift. Confinement in the xy plane should not play any significant role because of a rather large dot base size.

The atom intermixing (alloying) at the Si/Ge interface is considered as an additional reason which may contribute to the shift of the Ge-Ge mode towards lower frequencies due to the partial strain relaxation. The frequency position of the Ge-Si vibrational mode allows the atomic intermixing to be estimated. It strongly depends on the alloy composition while strain may induce minor shifts to lower frequency of 3 cm^{-1} [9]. Raman spectra of the investigated samples measured in both scattering geometries in the spectral range of the Ge-Si vibrations are shown in the Figure 4. The feature in the Raman spectrum of the sample A at 423 cm^{-1} corresponds to the Ge-Si vibrational mode existing at an almost abrupt interface, *i.e.* negligible intermixing, in an ideally strained superlattice [17]. Its frequency position is shifted markedly towards lower frequencies for the samples with QDs. One

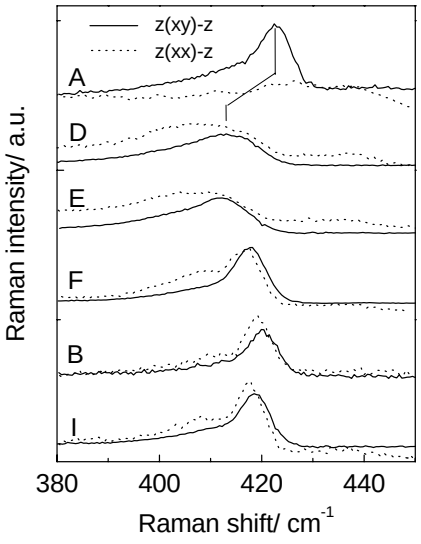

Fig. 4. Raman spectra of the samples A-I measured in $z(xy)-z$ and $z(xx)-z$ geometries in the spectral range of the Ge-Si vibrations (solid and dotted lines, respectively) at a temperature of 80 K.

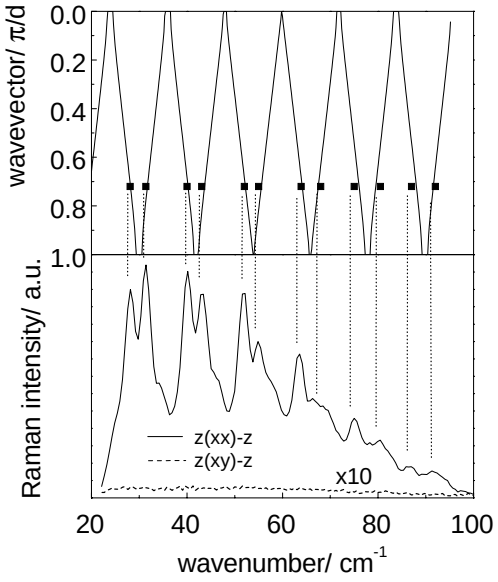

Fig. 5. Raman spectra of the sample K measured in $z(xx)-z$ and $z(xy)-z$ geometries in the in the acoustical spectral range (lower panel). The top panel shows the calculated dispersion of LA phonons.

can see that the difference in the frequency position of this mode for the samples A and D,E is about 11 cm^{-1} which is obviously much larger than the strain contribution mentioned above. Therefore, atomic intermixing in the interface region is very likely to be responsible for the shift of the interfacial Si-Ge vibrational mode and causes an additional shift of the Ge-Ge mode because of strain relaxation in an interfacial region. Assuming that a graded interface-involving in two atomic layer is formed and taking the masses of atoms at the Si-Ge and Ge-Si interfaces as $m_{\mathrm{Si-Ge}} = (1-x)\,m_{\mathrm{Ge}} + x\,m_{\mathrm{Si}}$ and $m_{\mathrm{Ge-Si}} = (1-x)\,m_{\mathrm{Si}} + x\,m_{\mathrm{Ge}}$ the maximal intermixing was estimated as $x = 0.09$ in samples D, E and $x = 0.04$ in sample F, B, I [9]. The shoulder observed at the low frequency side in the Raman spectra measured in $z(xx)-z$ geometry can be explained on the basis of theoretical calculations of interface intermixing by transverse optical vibrations which appear due to LO-TO splitting of the alloy-like Ge-Si vibrational modes [17].

Taking into account all these factors it allows the strain in the samples to be estimated. For the case of samples F, B, I the experimentally observed shift reaches a value of 15 cm^{-1} (Fig. 3) that corresponds to almost fully strained Ge QDs. The compressive strain of Ge bonds estimated from this shift using equation (2) is 4%. The strain in samples D and E is partially relaxed in the interface region with $x = 0.09$ and corresponds to 2.8%.

3.2 Acoustical region

As mentioned above the folded acoustic phonons in semiconductor superlattices are well investigated and understood. Nevertheless, data on the behaviour of acoustic phonons in structures with quantum dots is still lacking. As far as we know the folded acoustical phonons were detected recently only in periodical structures containing GaAs and AlAs QDs in an InAs matrix [18]. Here we demonstrate our results concerning folded acoustic phonons in Ge QD superlattices.

Figure 5 and Figure 6 show the Raman spectra of samples C and K measured in the acoustical spectral range in $z(xx)-z$ and $z(xy)-z$ scattering geometries. In agreement with the selection rules Raman spectra measured in $z(xy)-z$ geometry are featureless. Folded LA phonons are observed up to 7th order in $z(xx)-z$ geometry. The frequencies of the observed doublets of all samples are shown in Table 2. Using (1) we calculated the dispersions of acoustic phonons which are also presented in Figures 5 and 6. The frequency positions of folded LA phonons were determined at a scattering wave vector of $q_{\mathrm{s}} \approx 4\pi n/\lambda_{\mathrm{L}} = 1.054 \times 10^6$ cm^{-1}, where λ_{L} is the laser line (514.5 nm), n is the refractive index ($n \approx 4.33$ for Ge and Si at 514.5 nm). The best agreement of calculated and experimental data was obtained for parameters $\rho_1 = 5.36$ g/cm^3, $\rho_2 = 2.33$ g/cm^3, $\nu_1 = 4.9 \times 10^5$ cm/s and $\nu_2 = 8.44 \times 10^5$ cm/s which are equal to those taken for the calculation of Si/Ge superlattices [11]. Period of structure obtained from the calculation is 229 Å and 238 Å for samples C and K, respectively, that exceeds the nominal thickness by about 10%. This discrepancy may be caused by a slight deviation of growth parameters during MBE process or by fluctuation of layer thicknesses due to formation of the Ge quantum dots. Nevertheless, one can see that the model of elastic continuum which is usually used for the description of the acoustic spectrum of

Table 2. The experimental frequency positions of the folded LA phonons in Ge/Si structures.

	Frequency position of the folded LA doublets/cm^{-1}													
sample	-1	$+1$	-2	$+2$	-3	$+3$	-4	$+4$	-5	$+5$	-6	$+6$	-7	$+7$
D	78	84												
E	57.4	64.4												
F	37	45	75	81										
A		28	40	51	62	74	84	95	104	125				
B		27		50	67	75	88	97						
I		-	34	43	53	61	71	77	92	100				
C	15.5	17.4	27	29	38.4	40.8	49.8	51.8	60.8	63.8	71.8	74.8	82.3	
K			28	31.4	40	43.1	52	55	63.9	68	75	80.5	87	92

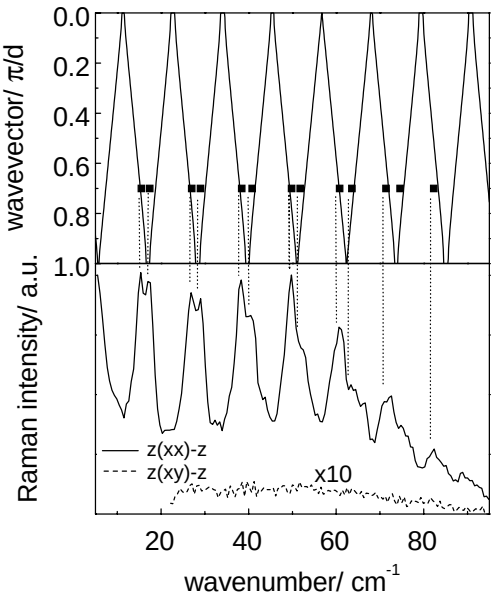

Fig. 6. Raman spectra of the sample C measured in $z(xx)-z$ and $z(xy)-z$ geometries in the acoustical spectral range. The top panel shows the calculated dispersion of LA phonons.

semiconductor superlattices is fairly well applicable to the periodical structures containing QDs.

4 Conclusion

We present the results of a Raman scattering study of self-organized Ge dot superlattices. The adequate description of the vibrational modes of these structures requires the confinement effect, strain and atomic intermixing to be taken into account. Strain and atomic intermixing in the structures was estimated from the analysis of Ge-Ge and Ge-Si phonon features. A number of doublets was observed in the acoustic spectral range which were assigned to the folded LA phonons. It was shown that the acoustic vibrations in the Ge dot superlattice can be well described by elastic continuum model.

References

1. U. Woggon, *Optical properties of Semiconductor quantum dots*, Springer Tracts in Modern Physics, V. 136 (Berlin, Heidelberg, 1997).
2. *Science and Engineering of One-and Zero-Dimensional Semiconductors*, Vol. 214, edited by S.P. Beaumont, C.N. Sotomayor-Torres (Plenum Press, New York, 1990).
3. J. Xu, H. Mao, Y. Du, J. Vac. Sci. Tecnol. B **15**, 1465 (1997).
4. G. Scamarcio, M. Lugara, D. Manno, Phys. Rev. B **45**, 13792 (1992).
5. P.V. Kamat, D. Meisel, *Semiconductors Nanoclusters*, V. 103 (Elsevier, New York, 1996).
6. D. Leonard, M.K. Krishnamurthy, C.M. Reeves, S.P. Denbaars, P.M. Petroff, Appl. Phys. Lett. **63**, 3203 (1993).
7. V.A. Markov, A.I. Nikiforov, O.P. Pchelyakov, J. Cryst. Growth **157**, 260 (1997).
8. A.I. Yakimov, A.V. Dvurechenskii, Yu.Yu. Proskuryakov, A.I. Nikiforov, O.P. Pchelyakov, S.A. Teys, A.K. Gutakovskii, Appl. Phys. Lett. **75**, 1413-1415 (1999).
9. M.W.C. Dharma-Wardana, G.C. Aers, D.J. Lockwood, J.-M. Baribeau, Phys. Rev. B **41**, 5319 (1990).
10. T. Ruf, *Phonon Raman Scattering in Semiconductors, Quantum Wells and Superlattices* (Springer-Verlag, Berlin, Heidelberg, 1998).
11. D.J. Lockwood, M.W.C. Dharma-Wardana, J.-M. Baribeau, D.C. Houghton, Phys. Rev. B **35**, 2243 (1987).
12. S.M. Rytov, Akoust. Zh. **2**, 71 (1956) [Sov. Phys. Acoust. **2**, 68 (1956)].
13. M. Seon, M. Holtz, T.-R. Park, O. Brafman, J.C. Bean, Phys. Rev. B **58**, 4779 (1998).
14. F. Cerdeira, C.J. Buchenauer, F.H. Pollak, M. Cardona, Phys. Rev. B **5**, 580 (1972).
15. S.H. Kwok, P.Y. Yu, C.H. Tung, Y.H. Zhang, M.F. Li, C.S. Peng, J.M. Zhou, Phys. Rev. B **59**, 4980 (1999).
16. *Light Scattering in Solids V*, edited by M. Cardona, G. Güntherodt (Springer-Verlag, Berlin, 1989).
17. S. de Gironcoli, E. Molinari, R. Schorer, G. Abstreiter, Phys. Rev. B **48**, 8959 (1993).
18. D. Tenne, V. Haisler, A. Toropov, A. Bakarov, A. Gutakovsky, D.R.T. Zahn, A. Shebanin, Phys. Rev. B (in press).